PERGAMON

International Journal of Solids and Structures 40 (2003) 5353–5370

INTERNATIONAL JOURNAL OF SOLIDS and STRUCTURES

www.elsevier.com/locate/ijsolstr

Electro-elastic interaction between a piezoelectric screw dislocation and circular interfacial rigid lines

Y.W. Liu *, Q.H. Fang

Department of Engineering Mechanics, Hunan University, Changsha 410082, People's Republic of China

Received 30 October 2002; received in revised form 7 April 2003

Abstract

The electro-elastic interaction between a piezoelectric screw dislocation located either outside or inside inhomogeneity and circular interfacial rigid lines under anti-plane mechanical and in-plane electrical loads in linear piezoelectric materials is dealt with in the framework of linear elastic theory. Using Riemann–Schwarz's symmetry principle integrated with the analysis of singularity of complex functions, the general solution of this problem is presented in this paper. For a special example, the closed form solutions for electro-elastic fields in matrix and inhomogeneity regions are derived explicitly when interface containing single rigid line. Applying perturbation technique, perturbation stress and electric displacement fields are obtained. The image force acting on piezoelectric screw dislocation is calculated by using the generalized Peach–Koehler formula. As a result, numerical analysis and discussion show that soft inhomogeneity can repel screw dislocation in piezoelectric material due to their intrinsic electro-mechanical coupling behavior and the influence of interfacial rigid line upon the image force is profound. When the radian of circular rigid line reaches extensive magnitude, the presence of interfacial rigid line can change the interaction mechanism.

Keywords: Piezoelectric materials; Image force; Interfacial rigid lines; Screw dislocation

1. Introduction

Due to this intrinsic coupling behavior, piezoelectric materials are used widely in modern technology such as high power sonar transducers, electro-mechanical actuator, piezoelectric power supplies and micro-positioner. These devices are designed to work under combined electro-mechanical loads. The presence of various defects, such as dislocations, cracks and inclusions, can greatly influence their characteristics and coupled behavior. Therefore, it is of vital importance to study the electro-elastic fields as a result of the presence of defects and inhomogeneities in these quasi-brittle solids.

Piezoelectric composites have become an important branch of modern engineering materials with fast development of the intelligent materials and structures. A number of contributions had been conducted on electro-elastic coupling characteristics of piezoelectric composite materials. Pak (1992) studied

* Corresponding author. Tel.: +86-731-8821889; fax: +86-731-8822330.
E-mail address: liuyouw8294@sina.com (Y.W. Liu).

0020-7683/$ - see front matter © 2003 Elsevier Ltd. All rights reserved.
doi:10.1016/S0020-7683(03)00287-7

the anti-plane problem of a piezoelectric circular inclusion. Meggiud and Zhong (1997) provided a general solution for the elliptical inhomogeneity problem in piezoelectric material under anti-plane shear and in-plane electric field. Kattis et al. (1998) investigated the electro-elastic interaction effects of a piezoelectric screw dislocation with circular inclusion in piezoelectric material. Meguid and Deng (1998) and Deng and Meguid (1999) considered the interaction between the piezoelectric elliptical inhomogeneity and a screw dislocation located inside inhomogeneity and outside inhomogeneity respectively under anti-plane shear and in-plane electric field. Recently, Huang and Kuang (2001) evaluated the generalized electro-mechanical force when dislocation located inside, outside and on the interface of elliptical inhomogeneity in a infinite piezoelectric media.

Above investigations and analysis all based on perfect interface between matrix and inclusion. Interfacial defects, typically interfacial cracks and interfacial rigid lines, can be produced inevitably in manufacturing and using of composite materials. Therefore, investigation on interaction of piezoelectric dislocation and inhomogeneity containing interfacial defects has important practical values which cannot only help to understand coupled electro-elastic characteristics of piezoelectric materials, but also offer scientific basis for the establishment of intelligent composites interface fracture criterion. The interaction of a screw dislocation and a thin film-covered crack in order to investigate the effects of a passive film on stress-corrosion cracking had been studied by Zhang and Qian (1996). Zhong and Meggiud (1997) studied the partially debonded circular inhomogeneity problem in piezoelectric materials under anti-plane shear and in-plane electric field. Lee et al. (2000) obtained the general solutions for a piezoelectric screw dislocation interacting with a semi-infinite crack. Detailed review of recent developments in fracture mechanics of piezoelectric materials can be found in the review paper by Zhang et al. (2001).

In this article, the electro-elastic interaction between a piezoelectric screw dislocation and circular inhomogeneity interfacial rigid lines under combined longitudinal shear and in-plane electric field is dealt with. Using Riemann–Schwarz's symmetry principle (Toya, 1974) integrated with the analysis singularity of complex functions (Liu, 1991), we present the general elastic solution of this problem and the closed form solution for interface containing a single rigid line inclusion. The holomorphic expressions of electro-elastic fields in matrix and inhomogeneity regions and image force are derived explicitly, and the influence of rigid line inclusion upon force acting on dislocation is discussed and shown graphically. Results presented in this paper contain the previous known solutions as special cases.

2. Basic formulation and problem statement

Assuming that the transversely isotropic piezoelectric media which has been poled along the z-direction with an isotropic xoy-plane, is subjected to remote longitudinal shear and in-plane electric field, then only coupled out-of-plane displacement and in-plane electric field need be considered so that there are only non-trivial displacement w, strains γ_{xz} and γ_{yz}, stresses τ_{xz} and τ_{yz}, electric potential φ, electrical field components E_x and E_y, electric displacement components D_x and D_y in the Cartesian coordinates. All components are only functions of variables of x and y. The mechanical and electric coupled constitutive equations (Tiersten (1969)) can be expressed as:

$$\tau_{xz} = C_{44}\frac{\partial w}{\partial x} + e_{15}\frac{\partial \varphi}{\partial x} \quad \tau_{yz} = C_{44}\frac{\partial w}{\partial y} + e_{15}\frac{\partial \varphi}{\partial y} \tag{1}$$

$$D_x = e_{15}\frac{\partial w}{\partial x} - d_{11}\frac{\partial \varphi}{\partial x} \quad D_y = e_{15}\frac{\partial w}{\partial y} - d_{11}\frac{\partial \varphi}{\partial y} \tag{2}$$

where C_{44} is the longitudinal shear modulus at a constant electric field, e_{15} is the piezoelectric modulus, d_{11} is the dielectric modulus at a constant stress field.

The equilibrium equation and charge equation can be reduced to the harmonic equations

$$\nabla^2 w = 0 \quad \nabla^2 \varphi = 0 \tag{3}$$

where $\nabla^2 = \partial^2/\partial x^2 + \partial^2/\partial y^2$ is Laplace operator.

Referring to the work by Jiang et al. (2001), we introduce the vector of generalized displacement $\mathbf{U} = \begin{Bmatrix} w \\ \varphi \end{Bmatrix}$. Substituting it into Eq. (3), we obtain

$$\nabla^2 \mathbf{U} = 0 \tag{4}$$

We introduce the vectors of generalized stress and strain.

$$\mathbf{\Sigma}_x = \begin{Bmatrix} \tau_{xz} \\ D_x \end{Bmatrix} \quad \mathbf{\Sigma}_y = \begin{Bmatrix} \tau_{yz} \\ D_y \end{Bmatrix} \tag{5}$$

$$\mathbf{Y}_x = \begin{Bmatrix} \gamma_{xz} \\ -E_x \end{Bmatrix} \quad \mathbf{Y}_y = \begin{Bmatrix} \gamma_{yz} \\ -E_y \end{Bmatrix} \tag{6}$$

By adopting the above notations, Eqs. (1) and (2) can be unified into

$$\mathbf{\Sigma}_x = M\mathbf{Y}_x \quad \mathbf{\Sigma}_y = M\mathbf{Y}_y \tag{7}$$

where

$$M = \begin{bmatrix} C_{44} & e_{15} \\ e_{15} & -d_{11} \end{bmatrix}$$

can be called the electro-elasticity modulus matrix.

Eq. (4) shows that the general solution of the generalized displacement vector $\mathbf{U}$ can be expressed by a generalized analytical function vector $\mathbf{f}(z)$, where $z = x + \mathrm{i}y$ is the complex variable.

$$\mathbf{U} = \mathrm{Re}\,\mathbf{f}(z) \tag{8}$$

where Re denotes the real part, and

$$\mathbf{f}(z) = \begin{Bmatrix} f_w(z) \\ f_\varphi(z) \end{Bmatrix} \tag{9}$$

$f_w(z)$ and $f_\varphi(z)$ are conventional analytical functions. By using the complex potential vector, the constitutive Eq. (7) can be expressed as

$$\mathbf{\Sigma}_x - \mathrm{i}\mathbf{\Sigma}_y = M\mathbf{F}(z) \tag{10}$$

where $\mathbf{F}(z) = \mathbf{f}'(z)$ and the superscript prime denotes derivative with respect to z. In term of polar coordinates r and ρ, Eq. (10) can be expressed as

$$\mathbf{\Sigma}_r - \mathrm{i}\mathbf{\Sigma}_\rho = \mathrm{e}^{\mathrm{i}\rho} M\mathbf{F}(z) \tag{11}$$

The problem to consider is as follows. Referring to Fig. 1, let piezoelectric medium I with electro-elasticity modulus M_1 occupy the region S^+, interior to the circle of radius R, while piezoelectric medium II with electro-elasticity modulus M_2 occupy region S^-, exterior the circle. A piezoelectric screw dislocation $\mathbf{b} = \{b_z, b_\varphi\}^{\mathrm{T}}$ is located at arbitrary point z_0 inside region S^- (or region S^+). Longitudinal shear stresses τ_{xz}^{∞}

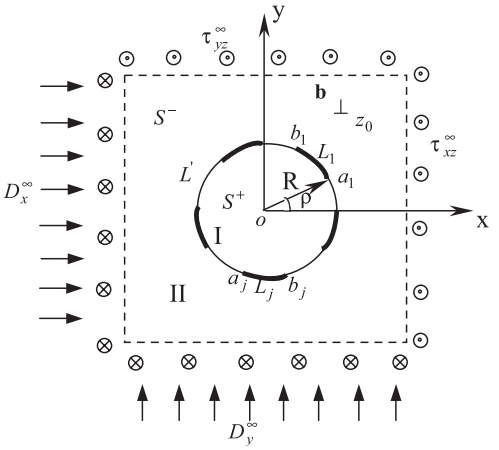

Fig. 1. Interaction of piezoelectric screw dislocation and circular interfacial rigid lines model.

and τ_{yz}^{∞} as well as electric displacements D_x^{∞} and D_y^{∞} are applied at infinite. A series of electrically conducting interfacial curvilinear rigid lines lie along a part L of the interface between two materials, where L is a union of rigid line segments L_j with the end points a_j and b_j $(j = 1, 2, \ldots, n)$. L' is the remainder of the interface which the inhomogeneity and the matrix are perfectly bonded.

Let the center of circle be placed at the origin of complex plane $z = x + \mathrm{i}y$ and $t = R\mathrm{e}^{\mathrm{i}\rho}$ be those points of z on $|z| = R$. The boundary conditions of generalized displacements and radial generalized stresses for the above problem can be expressed as follows:

$$\mathbf{U}_1^+(t) = \mathbf{U}_2^-(t) = \begin{Bmatrix} \delta_j \\ \varphi_j \end{Bmatrix} \quad t \in l_j \ (j = 1, 2, \ldots, n) \tag{12}$$

where δ_j is constant denoting a small anti-plane displacement of any rigid line l_j, φ_j is the electric potential on l_j.

$$\mathbf{\Sigma}_{r1}^+(t) = \mathbf{\Sigma}_{r2}^-(t) \quad t \in L' \tag{13}$$

$$\mathbf{U}_1^+(t) = \mathbf{U}_2^-(t) \quad t \in L' \tag{14}$$

After taking the derivatives with respect to ρ, the addition and subtraction of Eq. (12) yield

$$\mathbf{U}_1'^+(t) + \mathbf{U}_2'^-(t) = 0 \quad t \in L \tag{15}$$

$$\mathbf{U}_1'^+(t) - \mathbf{U}_2'^-(t) = 0 \quad t \in L \tag{16}$$

where the subscripts 1 and 2 denote the quantities defined in the region S^+ and S^-, with the superscripts + and − used to denoting the boundary values of the physical quantities as they approached from S^+ and S^-, respectively.

In addition to determine the unknown coefficients in the solution for such a problem, the equilibrium condition of each rigid line must be considered. Assuming that rigid lines are external traction and charge free, we have

$$\int_{a_j}^{b_j} \mathbf{\Sigma}_{r1}^+(t) \frac{\mathrm{d}t}{t} - \int_{a_j}^{b_j} \mathbf{\Sigma}_{r2}^-(t) \frac{\mathrm{d}t}{t} = 0 \quad j = 1, 2, \ldots, n \tag{17}$$

3. General solution of problem

3.1. A piezoelectric screw dislocation in matrix

3.1.1. General solution

Assuming that a piezoelectric screw dislocation is located in region S^- and considering Eq. (8), it is easy to obtain:

$$\mathbf{U}_2 = \mathrm{Re}\,\mathbf{f}_2(z) \tag{18}$$

Referring to the work by Pak (1990) and Jiang et al. (2001), the generalized analytical function vector $\mathbf{F}_2(z)$ in region S^- under considerations can be written as

$$\mathbf{F}_2(z) = \frac{1}{2\pi \mathrm{i}}\mathbf{b}\frac{1}{z-z_0} + \mathbf{\Gamma} + \mathbf{F}_{20}(z) \quad z \in S^- \tag{19}$$

where $\mathbf{F}_{20}(z)$ is holomorphic in region S^-, $\mathbf{b} = \begin{Bmatrix} b_z \\ b_\varphi \end{Bmatrix}$ is piezoelectric screw dislocation vector, $\mathbf{\Gamma}$ is determined from the far-field loads.

$$\mathbf{\Gamma} = M_2^{-1}(\mathbf{\Sigma}_x^\infty - \mathrm{i}\mathbf{\Sigma}_y^\infty) = M_2^{-1}\begin{bmatrix} \tau_{xz}^\infty - \mathrm{i}\tau_{yz}^\infty \\ D_x^\infty - \mathrm{i}D_y^\infty \end{bmatrix} \tag{20}$$

where

$$M_2 = \begin{bmatrix} C_{44}^{(2)} & e_{15}^{(2)} \\ e_{15}^{(2)} & -d_{11}^{(2)} \end{bmatrix}$$

superscript -1 denotes the inverse of a matrix.

Applying Riemann–Schwarz's symmetry principle and noting $t\bar{t} = R^2$ on $|z| = R$, we extend the definition of the holomorphic function $\mathbf{F}_2(z)$ into region S^+ lying along L by substitution

$$\mathbf{F}_2(z) = \frac{R^2}{z^2}\overline{\mathbf{F}}_2\left(\frac{R^2}{z}\right) \quad z \in S^+ \tag{21}$$

$\mathbf{F}_2(z)$ is holomorphic in region S^+, except at the points $z = R^2/z_0$ and $z = 0$ where it is singular. Using Eqs. (19) and (21), $\mathbf{F}_2(z)$ can be expressed as

$$\mathbf{F}_2(z) = \frac{1}{2\pi \mathrm{i}}\mathbf{b}\left(\frac{1}{z-z_0} + \frac{1}{z-z^*} - \frac{1}{z}\right) + \mathbf{\Gamma} + \frac{R^2}{z^2}\overline{\mathbf{\Gamma}} + F_{20}(z) \tag{22}$$

where $z^* = R^2/\bar{z}_0$ and $\mathbf{F}_{20}(z)$ is holomorphic over the entire plane cut along with L'.

$\mathbf{F}_1(z)$ is holomorphic in region S^+ and has form

$$\mathbf{F}_1(z) = \mathbf{D} + \mathbf{F}_{10}(z) \tag{23}$$

where $\mathbf{D}$ is a constant vector to be determined and $\mathbf{F}_{10}(z) = \mathrm{O}(1/z)$ near $z = 0$.

Similarly, extending function $\mathbf{F}_1(z)$ from S^+ to S^-, for large value of $|z|$, we obtain

$$\mathbf{F}_1(z) = \frac{R^2}{z^2}\overline{\mathbf{D}} + \mathrm{O}\left(\frac{1}{z^3}\right) \tag{24}$$

From Eqs. (14) and (16), it is seen that

$$\mathbf{U}_1'^+(t) = \mathbf{U}_2'^-(t) \quad t \in L + L' \tag{25}$$

at every point of entire circular boundary. After taking derivatives with respect to θ, and considering Eq. (8), the generalized displacement continuity condition (25) is written as

$$[\mathbf{F}_1(t)+\mathbf{F}_2(t)]^+ = [\mathbf{F}_1(t)+\mathbf{F}_2(t)]^- \quad t \in L + L' \tag{26}$$

Noting Eqs. (19), (22), (23) and (24) and according to the generalized Liouville's theorem, Eq. (26) leads to

$$\mathbf{F}_1(z)+\mathbf{F}_2(z) = \frac{1}{2\pi \mathrm{i}}\mathbf{b}G(z) + \left(\mathbf{\Gamma} + \frac{R^2}{z^2}\overline{\mathbf{\Gamma}}\right) \tag{27}$$

with

$$G(z) = \left(\frac{1}{z-z_0} + \frac{1}{z-z^*} - \frac{1}{z}\right)$$

Substituting Eq. (11) into Eq. (13), we obtain

$$M_1[\mathbf{F}_1^+(t)+\mathbf{F}_1^-(t)] = M_2[\mathbf{F}_2^+(t)+\mathbf{F}_2^-(t)] \quad t \in L' \tag{28}$$

Inserting Eq. (27) into Eq. (28), we have

$$\mathbf{F}_1^+(t)+\mathbf{F}_1^-(t) = \mathbf{N}_1 G(t) + 2(M_1+M_2)^{-1}M_2\left(\mathbf{\Gamma} + \frac{R^2}{t^2}\overline{\mathbf{\Gamma}}\right) \quad t \in L' \tag{29}$$

with $\mathbf{N}_1 = (1/\pi\mathrm{i})(M_1+M_2)^{-1}M_2\mathbf{b}$.

According to Muskhelishvili (1975), the general solution of Eq. (29) can be written as

$$\mathbf{F}_1(z) = \frac{X_0(z)}{2\pi \mathrm{i}}\int_L \frac{\mathbf{h}(t)}{X_0^+(t)(t-z)}\,\mathrm{d}t + X_0(z)\mathbf{P}_n(z) \tag{30}$$

where $\mathbf{h}(t) = \mathbf{N}_1 G(t) + 2(M_1+M_2)^{-1}M_2\left(\mathbf{\Gamma} + \frac{R^2}{t^2}\overline{\mathbf{\Gamma}}\right)$

$$\begin{aligned} \mathbf{P}_n(z) &= \begin{bmatrix} \sum_{j=1}^n C_j^{(w)} z^{n-j} \\ \sum_{j=1}^n C_j^{(\varphi)} z^{n-j} \end{bmatrix} \\ X_0(z) &= \prod_{j=1}^n (z-a_j)^{-1/2}(z-b_j)^{-1/2} \end{aligned} \tag{31}$$

$X_0(z)$ is a single-valued branch in the plane cut along with L' and for which

$$\lim_{|z|\to\infty} z^n X_0(z) = 1 \tag{32}$$

After evaluating the Cauchy integral in Eq. (30), we obtain

$$\mathbf{F}_1(z) = X_0(z)\left\{\mathbf{P}_n(z) - \frac{1}{2}[\mathbf{h}_0(z)+\mathbf{h}_\infty(z)+\mathbf{h}_{z_0}(z)+\mathbf{h}_{z^*}(z)]\right\} + \frac{1}{2}\mathbf{h}(z) \tag{33}$$

where $\mathbf{h}_0(z), \mathbf{h}_\infty(z), \mathbf{h}_{z_0}(z)$ and $\mathbf{h}_{z^*}(z)$ represent the principal parts at the points $z=0, z=\infty, z=z_0$ and $z=z^*$ of function $\mathbf{h}(z)/X_0(z)$, respectively.

The remaining integration constants in Eq. (30) are determined from the equilibrium conditions (17) of the rigid lines. Noting Eq. (11), we obtain $2n$ closed contour integrals

$$\int_{\wedge_j} [M_1\mathbf{F}_1(z) + M_2\mathbf{F}_2(z)]\,\mathrm{d}z = 0 \quad j = 1,2,\ldots,n \tag{34}$$

where $\wedge_j$ is a closed contour encircling each rigid line L_j with the poles $(z=0, z_0, z^*)$ outside contour.

Considering Eq. (27), Eq. (34) can be expressed as follows

$$\int_{\wedge_j}\left[(M_1-M_2)\mathbf{F}_1(z)+\frac{1}{2\pi\mathrm{i}}M_2\mathbf{b}G(z)+M_2\left(\mathbf{\Gamma}+\frac{R^2}{z^2}\overline{\mathbf{\Gamma}}\right)\right]\mathrm{d}z=0\quad j=1,2,\ldots,n \tag{35}$$

This is a system of $2n$ linear algebraic equations solving for the unknown constants. Substituting Eq. (33) into Eq. (35), the remaining integration constants can be determined. Once $\mathbf{F}_1(z)$ is available, $\mathbf{F}_2(z)$ will be simply obtained from Eq. (27).

3.1.2. Typical solution

As a typical case, we consider the problem of interface containing single rigid line. Further more, let us consider the case of the rigid line symmetrically placed with respected to the x-axis which ends are located at $a=R\mathrm{e}^{-\mathrm{i}\theta}$ and $b=R\mathrm{e}^{\mathrm{i}\theta}$ on $|z|=R$ as shown in Fig. 2.

In this case, $\mathbf{P}_n(z)$ and $X_0(z)$ have form

$$\mathbf{P}_1(z)=\begin{bmatrix}C_1^{(w)} & C_1^{(\varphi)}\end{bmatrix}^{\mathrm{T}} \tag{36}$$

$$X_0(z)=(z-a)^{-1/2}(z-b)^{-1/2} \tag{37}$$

Expanding $1/X_0(z)$ into Laurent series in the vicinity of $z=0$ and $|z|=\infty$, and noting $X_0(0)=(1/R)$, we obtain

$$\mathbf{h}_0(z)=-\frac{R}{z}\mathbf{N}_1+2(M_2+M_1)^{-1}M_2\left(-\frac{R^2}{z}\cos\theta\overline{\mathbf{\Gamma}}+\frac{R^3}{z^2}\overline{\mathbf{\Gamma}}\right) \tag{38}$$

$$\mathbf{h}_\infty(z)=\mathbf{N}_1+2(M_2+M_1)^{-1}M_2(\mathbf{\Gamma}z-\mathbf{\Gamma}R\cos\theta) \tag{39}$$

$$\mathbf{h}_{z_0}(z)=\mathbf{N}_1\frac{\sqrt{(z_0-a)(z_0-b)}}{z-z_0} \tag{40}$$

$$\mathbf{h}_{z^*}(z)=\mathbf{N}_1\frac{\sqrt{(z^*-a)(z^*-b)}}{z-z^*} \tag{41}$$

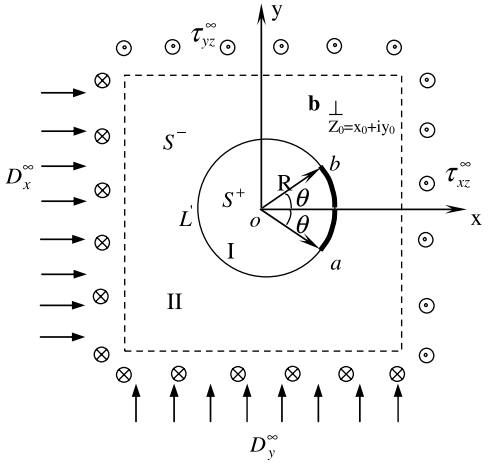

Fig. 2. Interface containing single rigid line.

Substituting Eqs. (38)–(41) into Eq. (33), and applying the residue theorem, the unknown coefficient can be calculated:

$$\begin{bmatrix} C_1^{(w)} \\ C_1^{(\varphi)} \end{bmatrix} = \begin{bmatrix} 0 \\ 0 \end{bmatrix} \tag{42}$$

Substituting Eqs. (38)–(41) into Eq. (33), and considering Eq. (42), the general solution of $\mathbf{F}_1(z)$ can be written as

$$\begin{aligned}\mathbf{F}_1(z) = {} & (M_1+M_2)^{-1}M_2\left(\mathbf{\Gamma}+\frac{R^2}{t^2}\overline{\mathbf{\Gamma}}\right)+(M_2+M_1)^{-1}M_2\left(\frac{R^2}{z}\cos\theta\overline{\mathbf{\Gamma}}-\frac{R^3}{z^2}\overline{\mathbf{\Gamma}}-\mathbf{\Gamma}z+\mathbf{\Gamma}R\cos\theta\right)\\ & \times\frac{1}{\sqrt{(z-a)(z-b)}}+\frac{1}{2\pi\mathrm{i}}(M_1+M_2)^{-1}M_2\mathbf{b}\left(\frac{1}{z-z_0}+\frac{1}{z-z^*}-\frac{1}{z}\right)-\frac{1}{2\pi\mathrm{i}}(M_1+M_2)^{-1}M_2\mathbf{b}\\ & \times\left(\frac{\sqrt{(z_0-a)(z_0-b)}}{z-z_0}+\frac{\sqrt{(z^*-a)(z^*-b)}}{z-z^*}-\frac{R}{z}+1\right)\frac{1}{\sqrt{(z-a)(z-b)}}\end{aligned} \tag{43}$$

The function $\mathbf{F}_2(z)$ can be found by substituting Eq. (33) into Eq. (27), it is

$$\begin{aligned}\mathbf{F}_2(z) = {} & (M_1+M_2)^{-1}M_1\left(\mathbf{\Gamma}-\frac{R^2}{t^2}\overline{\mathbf{\Gamma}}\right)-(M_2+M_1)^{-1}M_2\left(\frac{R^2}{z}\cos\theta\overline{\mathbf{\Gamma}}-\frac{R^3}{z^2}\overline{\mathbf{\Gamma}}-\mathbf{\Gamma}z+\mathbf{\Gamma}R\cos\theta\right)\\ & \times\frac{1}{\sqrt{(z-a)(z-b)}}+\frac{1}{2\pi\mathrm{i}}(M_1+M_2)^{-1}M_1\mathbf{b}\left(\frac{1}{z-z_0}+\frac{1}{z-z^*}-\frac{1}{z}\right)+\frac{1}{2\pi\mathrm{i}}(M_1+M_2)^{-1}M_2\mathbf{b}\\ & \times\left(\frac{\sqrt{(z_0-a)(z_0-b)}}{z-z_0}+\frac{\sqrt{(z^*-a)(z^*-b)}}{z-z^*}-\frac{R}{z}+1\right)\frac{1}{\sqrt{(z-a)(z-b)}}\end{aligned} \tag{44}$$

The solution to the problem of corresponding homogeneous material containing single circular-arc rigid line is the special case as $M_1 = M_2$, which is

$$\begin{aligned}\mathbf{F}(z) = {} & \frac{1}{2}\left(\mathbf{\Gamma}+\frac{R^2}{t^2}\overline{\mathbf{\Gamma}}\right)-\frac{1}{2}\left(\frac{R^2}{z}\cos\theta\overline{\mathbf{\Gamma}}-\frac{R^3}{z^2}\overline{\mathbf{\Gamma}}-\mathbf{\Gamma}z+\mathbf{\Gamma}R\cos\theta\right)\frac{1}{\sqrt{(z-a)(z-b)}}\\ & +\frac{1}{4\pi\mathrm{i}}\mathbf{b}\left(\frac{1}{z-z_0}+\frac{1}{z-z^*}-\frac{1}{z}\right)+\frac{1}{4\pi\mathrm{i}}\mathbf{b}\left(\frac{\sqrt{(z_0-a)(z_0-b)}}{z-z_0}+\frac{\sqrt{(z^*-a)(z^*-b)}}{z-z^*}-\frac{R}{z}+1\right)\\ & \times\frac{1}{\sqrt{(z-a)(z-b)}}\end{aligned} \tag{45}$$

This is a new solution.

Assuming $\theta = 0$ and $\Gamma = 0$, namely, radian of interfacial rigid line and generalized stresses at infinite are equal to zero; we obtain the solutions on interaction between a piezoelectric screw dislocation and circular inhomogeneity.

$$\mathbf{F}_1(z) = \frac{1}{\pi\mathrm{i}}(M_1+M_2)^{-1}M_2\mathbf{b}\frac{1}{z-z_0} \tag{46}$$

$$\mathbf{F}_2(z) = \frac{1}{2\pi\mathrm{i}}\mathbf{b}\frac{1}{z-z_0}+\frac{1}{2\pi\mathrm{i}}(M_1+M_2)^{-1}(M_1-M_2)\mathbf{b}\left(\frac{1}{z-z^*}-\frac{1}{z}\right) \tag{47}$$

which are identical to the results in Kattis et al. (1998) and Liu et al. (2000).

3.2. A piezoelectric screw dislocation inside the inhomogeneity

Assuming a screw dislocation is located inside inhomogeneity and vanishes at infinite, by the application of analysis of singularity of $\mathbf{F}(z)$, the complex potential in inhomogeneity region can be expressed as

$$\mathbf{F}_1(z) = \frac{1}{2\pi \mathrm{i}}\mathbf{b}\frac{1}{z - z_0} + \mathbf{F}_{10}(z) \quad z \in S^+ \tag{48}$$

where $\mathbf{F}_{10}(z)$ is a holomorphic complex function in region S^+.

The complex potential outside inhomogeneity is holomorpic and takes the following form for large value of $|z|$.

$$\mathbf{F}_2(z) = \frac{1}{2\pi \mathrm{i}}\mathbf{b}\frac{1}{z} + \mathrm{O}\left(\frac{1}{z^2}\right) \quad z \in S^- \tag{49}$$

Assuming interface containing single rigid line inclusion, furthermore, let the center of arc L lie on the positive x-axis and the central angle subtended by arc L be 2θ, using the same method introducing in Section 3.1, the complex potentials inside inhomogeneity and matrix can be expressed as follows:

$$\begin{aligned}\mathbf{F}_1(z) = {} & \frac{1}{2\pi \mathrm{i}}(M_1 + M_2)^{-1}M_2\mathbf{b}\left(\frac{1}{z - z_0} + \frac{1}{z - z^*} - \frac{1}{z}\right) + \frac{1}{2\pi \mathrm{i}}(M_1 + M_2)^{-1}M_1\mathbf{b} \\ & \times \left(\frac{\sqrt{(z_0 - a)(z_0 - b)}}{z - z_0} + \frac{\sqrt{(z^* - a)(z^* - b)}}{z - z^*}\right)\frac{1}{\sqrt{(z - a)(z - b)}} + \frac{1}{2\pi \mathrm{i}}(M_1 + M_2)^{-1}M_2\mathbf{b} \\ & \times \left(\frac{R}{z} - 1\right)\frac{1}{\sqrt{(z - a)(z - b)}}\end{aligned} \tag{50}$$

$$\begin{aligned}\mathbf{F}_2(z) = {} & \frac{1}{2\pi \mathrm{i}}(M_1 + M_2)^{-1}M_1\mathbf{b}\left(\frac{1}{z - z_0} + \frac{1}{z - z^*} - \frac{1}{z}\right) - \frac{1}{2\pi \mathrm{i}}(M_1 + M_2)^{-1}M_1\mathbf{b} \\ & \times \left(\frac{\sqrt{(z_0 - a)(z_0 - b)}}{z - z_0} + \frac{\sqrt{(z^* - a)(z^* - b)}}{z - z^*}\right)\frac{1}{\sqrt{(z - a)(z - b)}} - \frac{1}{2\pi \mathrm{i}}(M_1 + M_2)^{-1}M_2\mathbf{b} \\ & \times \left(\frac{R}{z} - 1\right)\frac{1}{\sqrt{(z - a)(z - b)}}\end{aligned} \tag{51}$$

Assuming the radian of rigid line θ is equal to zero and the piezoelectric coupling effect is absent, Eqs. (45) and (46) reduce to

$$F_1(z) = \frac{G_1 b_z}{2\pi \mathrm{i}}\frac{1}{z - z_0} + \frac{G_1(G_2 - G_1)b_z}{2\pi \mathrm{i}(G_1 + G_2)}\frac{1}{z - z^*} \tag{52}$$

$$F_2(z) = \frac{G_2(G_2 - G_1)b_z}{2\pi \mathrm{i}(G_1 + G_2)}\frac{1}{z} + \frac{G_1 G_2 b_z}{\pi \mathrm{i}(G_1 + G_2)}\frac{1}{z - z_0} \tag{53}$$

Eqs. (52) and (53) agree with the results of Smith (1968).

4. Stresses and electric displacements

Substituting Eqs. (43) and (44) into Eq. (10) respectively, stress fields and electric displacement fields in inhomogeneity and matrix can be evaluated.

$$\begin{aligned}\boldsymbol{\Sigma}_{x1}-\mathrm{i}\boldsymbol{\Sigma}_{y1}=&M_1(M_1+M_2)^{-1}M_2\left(\boldsymbol{\Gamma}+\frac{R^2}{z^2}\overline{\boldsymbol{\Gamma}}\right)+M_1(M_2+M_1)^{-1}M_2\left(\frac{R^2}{z}\cos\theta\overline{\boldsymbol{\Gamma}}-\frac{R^3}{z^2}\overline{\boldsymbol{\Gamma}}-\boldsymbol{\Gamma}z+\boldsymbol{\Gamma}R\cos\theta\right)\\&\times\frac{1}{\sqrt{(z-a)(z-b)}}+\frac{1}{2\pi\mathrm{i}}M_1(M_1+M_2)^{-1}M_2\mathbf{b}\left(\frac{1}{z-z_0}+\frac{1}{z-z^*}-\frac{1}{z}\right)-\frac{1}{2\pi\mathrm{i}}M_1(M_1+M_2)^{-1}M_2\mathbf{b}\\&\times\left(\frac{\sqrt{(z_0-a)(z_0-b)}}{z-z_0}+\frac{\sqrt{(z^*-a)(z^*-b)}}{z-z^*}-\frac{R}{z}+1\right)\frac{1}{\sqrt{(z-a)(z-b)}}\end{aligned}\tag{54}$$

$$\begin{aligned}\boldsymbol{\Sigma}_{x2}-\mathrm{i}\boldsymbol{\Sigma}_{y2}=&M_2(M_1+M_2)^{-1}M_1\left(\boldsymbol{\Gamma}+\frac{R^2}{z^2}\overline{\boldsymbol{\Gamma}}\right)-M_2(M_2+M_1)^{-1}M_2\left(\frac{R^2}{z}\cos\theta\overline{\boldsymbol{\Gamma}}-\frac{R^3}{z^2}\overline{\boldsymbol{\Gamma}}-\boldsymbol{\Gamma}z+\boldsymbol{\Gamma}R\cos\theta\right)\\&\times\frac{1}{\sqrt{(z-a)(z-b)}}+\frac{1}{2\pi\mathrm{i}}M_2(M_1+M_2)^{-1}M_1\mathbf{b}\left(\frac{1}{z-z_0}+\frac{1}{z-z^*}-\frac{1}{z}\right)+\frac{1}{2\pi\mathrm{i}}M_2(M_1+M_2)^{-1}M_2\mathbf{b}\\&\times\left(\frac{\sqrt{(z_0-a)(z_0-b)}}{z-z_0}+\frac{\sqrt{(z^*-a)(z^*-b)}}{z-z^*}-\frac{R}{z}+1\right)\frac{1}{\sqrt{(z-a)(z-b)}}\end{aligned}\tag{55}$$

When the dislocation is located inside the inhomogeneity, substituting Eqs. (50) and (51) into Eq. (10), we have

$$\begin{aligned}\boldsymbol{\Sigma}_{x1}-\mathrm{i}\boldsymbol{\Sigma}_{y1}=&\frac{1}{2\pi\mathrm{i}}M_1(M_1+M_2)^{-1}M_2\mathbf{b}\left(\frac{1}{z-z_0}+\frac{1}{z-z^*}-\frac{1}{z}\right)\\&+\frac{1}{2\pi\mathrm{i}}M_1(M_1+M_2)^{-1}M_1\mathbf{b}\left(\frac{\sqrt{(z_0-a)(z_0-b)}}{z-z_0}+\frac{\sqrt{(z^*-a)(z^*-b)}}{z-z^*}\right)\frac{1}{\sqrt{(z-a)(z-b)}}\\&+\frac{1}{2\pi\mathrm{i}}M_1(M_1+M_2)^{-1}M_2\mathbf{b}\left(\frac{R}{z}-1\right)\frac{1}{\sqrt{(z-a)(z-b)}}\end{aligned}\tag{56}$$

$$\begin{aligned}\boldsymbol{\Sigma}_{x2}-\mathrm{i}\boldsymbol{\Sigma}_{y2}=&\frac{1}{2\pi\mathrm{i}}M_2(M_1+M_2)^{-1}M_1\mathbf{b}\left(\frac{1}{z-z_0}+\frac{1}{z-z^*}-\frac{1}{z}\right)\\&-\frac{1}{2\pi\mathrm{i}}M_2(M_1+M_2)^{-1}M_1\mathbf{b}\left(\frac{\sqrt{(z_0-a)(z_0-b)}}{z-z_0}+\frac{\sqrt{(z^*-a)(z^*-b)}}{z-z^*}\right)\frac{1}{\sqrt{(z-a)(z-b)}}\\&-\frac{1}{2\pi\mathrm{i}}M_2(M_1+M_2)^{-1}M_2\mathbf{b}\left(\frac{R}{z}-1\right)\frac{1}{\sqrt{(z-a)(z-b)}}\end{aligned}\tag{57}$$

5. Image force

5.1. Perturbation stress and electric displacement at the dislocation

The perturbation stress and electric displacement components at the dislocation are obtained by subtracting those attribution to the dislocation in the corresponding infinite homogeneous medium from Eq. (55) or (56), then taking the limit for z approaches to z_0.

(1) Dislocation inside matrix

$$\begin{aligned}\boldsymbol{\Sigma}^0_{x2}-\mathrm{i}\boldsymbol{\Sigma}^0_{y2}=&M_2(M_1+M_2)^{-1}M_1\left(\boldsymbol{\Gamma}+\frac{R^2}{z_0^2}\overline{\boldsymbol{\Gamma}}\right)-M_2(M_2+M_1)^{-1}M_2\left(\frac{R^2}{z}\cos\theta\overline{\boldsymbol{\Gamma}}-\frac{R^3}{z^2}\overline{\boldsymbol{\Gamma}}-\boldsymbol{\Gamma}z+\boldsymbol{\Gamma}R\cos\theta\right)\\&\times\frac{1}{\sqrt{(z_0-a)(z_0-b)}}+\frac{1}{2\pi\mathrm{i}}M_2(M_1+M_2)^{-1}M_1\mathbf{b}\left(\frac{1}{z_0-z^*}-\frac{1}{z_0}\right)\\&+\frac{1}{2\pi\mathrm{i}}M_2(M_1+M_2)^{-1}M_2\mathbf{b}\left(\frac{\sqrt{(z^*-a)(z^*-b)}}{z_0-z^*}-\frac{R}{z_0}+1\right)\frac{1}{\sqrt{(z-a)(z-b)}}\\&-\frac{1}{4\pi\mathrm{i}}M_2(M_1+M_2)^{-1}M_2\mathbf{b}\left(\frac{1}{z_0-a}+\frac{1}{z_0-b}\right)\end{aligned}\tag{58}$$

(2) Dislocation inside inhomogeneity

$$\begin{aligned}\boldsymbol{\Sigma}^0_{x1}-\mathrm{i}\boldsymbol{\Sigma}^0_{y1}=&\frac{1}{2\pi\mathrm{i}}M_1(M_1+M_2)^{-1}M_2\mathbf{b}\left(\frac{1}{z_0-z^*}-\frac{1}{z_0}\right)+\frac{1}{2\pi\mathrm{i}}M_1(M_1+M_2)^{-1}M_1\mathbf{b}\left(\frac{\sqrt{(z^*-a)(z^*-b)}}{z_0-z^*}\right)\\&\times\frac{1}{\sqrt{(z_0-a)(z_0-b)}}+\frac{1}{2\pi\mathrm{i}}M_1(M_1+M_2)^{-1}M_2\mathbf{b}\left(\frac{R}{z_0}-1\right)\\&\times\frac{1}{\sqrt{(z_0-a)(z_0-b)}}-\frac{1}{4\pi\mathrm{i}}M_1(M_1+M_2)^{-1}M_1\mathbf{b}\left(\frac{1}{z_0-a}+\frac{1}{z_0-b}\right)\end{aligned}\tag{59}$$

5.2. Image force

Image force (Hirth and Lothe, 1982) on the dislocation is a significant physical quantum for understanding interacting mechanism in studying the interaction effects of piezoelectric dislocation and inhomogeneity. The image force can be obtained by using the generalized Peach–Keohler formula by Pak (1990) as follow

$$F_x-\mathrm{i}F_y=\mathrm{i}\mathbf{b}^{\mathrm{T}}\left(\boldsymbol{\Sigma}^0_{xk}-\mathrm{i}\boldsymbol{\Sigma}^0_{yk}\right)\quad(k=1,2)\tag{60}$$

Substituting Eq. (58) or (59) into Eq. (60), image force components F_x and F_y can be determined.

(1) Dislocation inside matrix at arbitrary point z_0.

$$\begin{aligned}F_x-\mathrm{i}F_y=&\mathrm{i}\mathbf{b}^{\mathrm{T}}M_2(M_1+M_2)^{-1}M_1\left(\boldsymbol{\Gamma}+\frac{R^2}{z_0^2}\overline{\boldsymbol{\Gamma}}\right)-\mathrm{i}\mathbf{b}^{\mathrm{T}}M_2(M_2+M_1)^{-1}M_2\\&\times\left(\frac{R^2}{z}\cos\theta\overline{\boldsymbol{\Gamma}}-\frac{R^3}{z^2}\overline{\boldsymbol{\Gamma}}-\boldsymbol{\Gamma}z+\boldsymbol{\Gamma}R\cos\theta\right)\frac{1}{\sqrt{(z_0-a)(z_0-b)}}+\mathbf{b}^{\mathrm{T}}M_2(M_1+M_2)^{-1}M_1\mathbf{b}\frac{1}{2\pi}\\&\times\left(\frac{1}{z_0-z^*}-\frac{1}{z_0}\right)+\mathbf{b}^{\mathrm{T}}M_2(M_1+M_2)^{-1}M_2\mathbf{b}\frac{1}{2\pi}\left(\frac{\sqrt{(z^*-a)(z^*-b)}}{z_0-z^*}-\frac{R}{z_0}+1\right)\\&\times\frac{1}{\sqrt{(z_0-a)(z_0-b)}}-\mathbf{b}^{\mathrm{T}}M_2(M_1+M_2)^{-1}M_2\mathbf{b}\frac{1}{4\pi}\left(\frac{1}{z_0-a}+\frac{1}{z_0-b}\right)\end{aligned}\tag{61}$$

(2) Dislocation inside inhomogeneity at arbitrary point z_0.

$$F_x - \mathrm{i}F_y = \mathbf{b}^{\mathrm{T}} M_1 (M_1 + M_2)^{-1} M_2 \mathbf{b} \frac{1}{2\pi} \left(\frac{1}{z_0 - z^*} - \frac{1}{z_0} \right) + \mathbf{b}^{\mathrm{T}} M_1 (M_1 + M_2)^{-1} M_1 \mathbf{b} \frac{1}{2\pi} \left(\frac{\sqrt{(z^* - a)(z^* - b)}}{z_0 - z^*} \right) \times \frac{1}{\sqrt{(z_0 - a)(z_0 - b)}} + \mathbf{b}^{\mathrm{T}} M_1 (M_1 + M_2)^{-1} M_2 \mathbf{b} \frac{1}{2\pi} \left(\frac{R}{z_0} - 1 \right) \times \frac{1}{\sqrt{(z_0 - a)(z_0 - b)}} - \mathbf{b}^{\mathrm{T}} M_1 (M_1 + M_2)^{-1} M_1 \mathbf{b} \frac{1}{4\pi} \left(\frac{1}{z_0 - a} + \frac{1}{z_0 - b} \right) \tag{62}$$

When $\theta = 0$ and $\Gamma = 0$, the corresponding image force between piezoelectric screw dislocation and circular elastic inhomogeneity is obtained from Eq. (61) which coincides with the result of Liu et al. (2000).

When dislocation lies on x-axis and generalized loads vanish at infinite, $z_0 = x_0$, $\Gamma = 0$, expressions (61) and (62) reduce to

(1) Dislocation inside matrix

$$F_x = \mathbf{b}^{\mathrm{T}} M_2 (M_1 + M_2)^{-1} M_1 \mathbf{b} \frac{1}{2\pi} \left(\frac{x_0}{x_0^2 - R^2} - \frac{1}{x_0} \right) + \mathbf{b}^{\mathrm{T}} M_2 (M_1 + M_2)^{-1} M_2 \mathbf{b} \times \frac{1}{2\pi} \left(\frac{\sqrt{(R^2 - x_0 a)(R^2 - x_0 b)}}{x_0^2 - R^2} - \frac{R}{x_0} + 1 \right) \frac{1}{\sqrt{(x_0 - a)(x_0 - b)}} - \mathbf{b}^{\mathrm{T}} M_2 (M_1 + M_2)^{-1} M_2 \mathbf{b} \times \frac{1}{4\pi} \left(\frac{1}{x_0 - a} + \frac{1}{x_0 - b} \right) \tag{63}$$

$$F_y = 0 \tag{64}$$

(2) Dislocation inside inhomogeneity

$$F_x = \mathbf{b}^{\mathrm{T}} M_1 (M_1 + M_2)^{-1} M_2 \mathbf{b} \frac{1}{2\pi} \left(\frac{x_0}{x_0^2 - R^2} - \frac{1}{x_0} \right) + \mathbf{b}^{\mathrm{T}} M_1 (M_1 + M_2)^{-1} M_1 \mathbf{b} \frac{1}{2\pi} \left(\frac{\sqrt{(R^2 - x_0 a)(R^2 - x_0 b)}}{x_0^2 - R^2} \right) \times \frac{1}{\sqrt{(x_0 - a)(x_0 - b)}} + \mathbf{b}^{\mathrm{T}} M_1 (M_1 + M_2)^{-1} M_2 \mathbf{b} \frac{1}{2\pi} \left(\frac{R}{x_0} - 1 \right) \frac{1}{\sqrt{(x_0 - a)(x_0 - b)}} - \mathbf{b}^{\mathrm{T}} M_1 (M_1 + M_2)^{-1} M_1 \mathbf{b} \frac{1}{4\pi} \left(\frac{1}{x_0 - a} + \frac{1}{x_0 - b} \right) \tag{65}$$

$$F_y = 0 \tag{66}$$

Above Eqs. (63)–(66) indicate image force component F_y equals to zero and the dislocation only moves along x-axis when dislocation lies on x-axis.

6. Numerical analysis and discussion

From Eqs. (61) and (62), we can discuss the influence of all parameters upon image force. For the convenience of comparing with previous known solutions, we analyze the special case when dislocation lies on x-axis in the absence of remote generalized loads. Assuming the piezoelectric screw dislocation vector (Lee et al., 2000)

$$\mathbf{b} = \begin{Bmatrix} b_z \\ b_\varphi \end{Bmatrix} = \begin{Bmatrix} 1.0 \times 10^{-9}\ \text{m} \\ 1.0\ \text{V} \end{Bmatrix}$$

and using Eqs. (63) and (65), the influence of circular interfacial crack upon image force is discussed as follows.

(1) Dislocation in matrix

Let us define the normalized force on dislocation as $F_{xo1} = (2\pi R/C_{44}^{(2)}b_z^2)F_x$. Assuming matrix material is PZT-5H piezoelectric ceramics with the electro-elastic properties:

$$M_2 = \begin{bmatrix} 3.53 \times 10^{10}\ \text{N/m}^2 & 17\ \text{C/m}^2 \\ 17\ \text{C/m}^2 & 1.51 \times 10^{-8}\ \text{C/Vm} \end{bmatrix}$$

and dielectric modulus $d_{11}^{(1)} = d_{11}^{(2)}$.

Let us introduce $\alpha_1 = C_{44}^{(1)}/C_{44}^{(2)}$, $\beta_1 = e_{15}^{(1)}/e_{15}^{(2)}$ and $\lambda_1 = R/x_0$. The normalized force F_{xo1} on dislocation versus θ is depicted in Fig. 3 with different β_1 for $\alpha_1 = 1$ and $\lambda_1 = 0.8$. It is seen that image force is equal to zero in homogeneous piezoelectric material as $\theta = 0$ and $\beta_1 = 1$. F_{xo1} is always positive as $\beta_1 > 1$, for which the piezoelectric inhomogeneity repel dislocation located inside matrix. For $\beta_1 < 1$, F_{xo1} is negative first, and then becomes positive. The image force will increase with the increase of rigid line angle θ which indicates interfacial rigid line repel piezoelectric screw dislocation. The variation of the normalized force F_{xo1} acting on dislocation with radian θ is plotted in Fig. 4 with different α for $\beta_1 = 2$ and $\lambda_1 = 0.8$. Noticeable, F_{xo1} is positive as $\theta = 0$ and $\alpha_1 = 0.1$, 0.8 which shows soft inhomogeneity can repel dislocation in piezoelectric materials due to their different piezoelectric constants ratio. To our knowledge, soft inhomogeneity will attract dislocation inside matrix all along in non-piezoelectric composites. It is also shown that F_{xo1} will increase with the increase of rigid line radian for which rigid line always repel dislocation. In Fig. 5, we illustrate variation of normalized force F_{xo1} versus λ_1 with different value of β_1 for $\alpha_1 = 1$ and $2\theta = 20°$. It is seen that the normalized force F_{xo1} is always positive as $\beta_1 > 1$. For $\beta_1 < 1$, circular piezoelectric inhomogeneity and rigid line inclusion attract dislocation first, and then repel it. There is a stable equilibrium position in x-axis and the image force equal to zero at that point. In spite of getting any value of β_1, the magnitude of repulsion force on dislocation will be a large value when dislocation approaches to inhomogeneity ($\lambda_1 \to 1$) from infinity along with x-axis. The variation of the normalized force F_{xo1} with λ_1 is plotted in Fig. 6 with different α_1 for $2\theta = 20°$ and $\beta_1 = 1$. It is seen that F_{xo1} is always positive when $\alpha_1 > 1$ (hard inhomogeneity), for which hard inhomogeneity and rigid line inclusion always repel dislocation

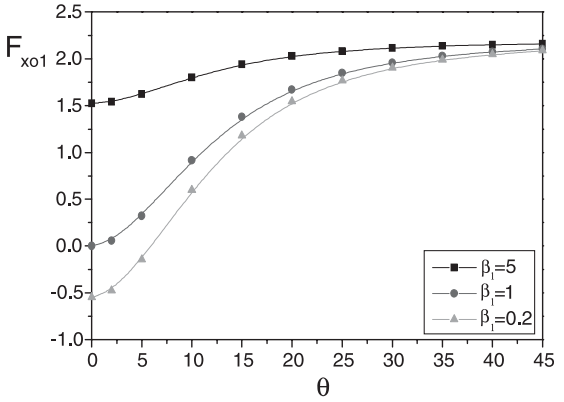

Fig. 3. Normalized force F_{xo1} versus θ with different β_1 for $\alpha_1 = 1$ and $\lambda_1 = 0.8$.

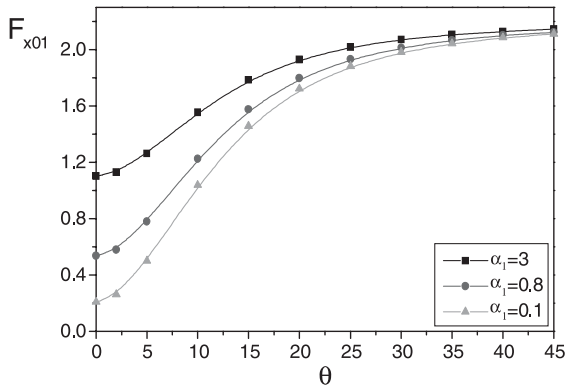

Fig. 4. Normalized force F_{xo1} versus θ with different α_1 for $\beta_1 = 2$ and $\lambda_1 = 0.8$.

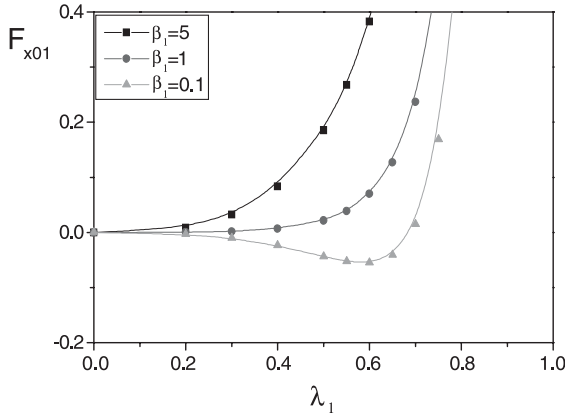

Fig. 5. Normalized force F_{xo1} versus λ_1 with different β_1 for $\alpha_1 = 1$ and $\theta = 10°$.

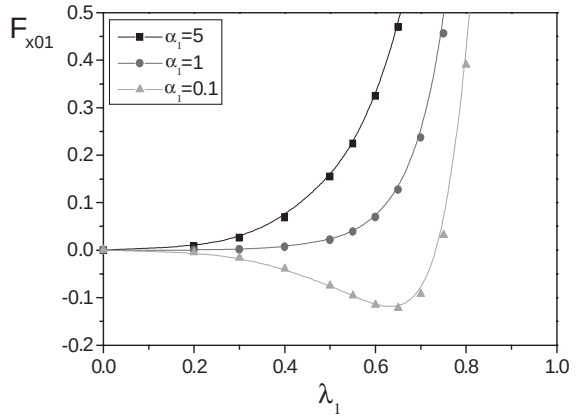

Fig. 6. Normalized force F_{xo1} versus λ_1 with different α_1 for $\beta_1 = 1$ and $\theta = 10°$.

located inside matrix. When $\alpha_1 < 1$ (soft inhomogeneity), the normalized force F_{xo1} is negative first, and then becomes positive as dislocation approaches to inhomogeneity from infinity along with x-axis. There also is a stable equilibrium position in x-axis and the image force equal to zero at that point. In spite of $\alpha_1 > 1$ or $\alpha_1 < 1$, the value of attraction force on dislocation will be a large value when dislocation approaches to rigid line inclusion.

(2) Dislocation inside inhomogeneity

Let us define the normalized force on dislocation as $F_{xo2} = (2\pi R/C_{44}^{(1)}b_z^2)F_x$. Assuming inhomogeneity material is PZT-5H piezoelectric ceramics with the electro-elastic properties:

$$M_1 = \begin{bmatrix} 3.53 \times 10^{10}\ \mathrm{N/m^2} & 17\ \mathrm{C/m^2} \\ 17\ \mathrm{C/m^2} & 1.51 \times 10^{-8}\ \mathrm{C/Vm} \end{bmatrix}$$

and dielectric modulus $d_{11}^{(1)} = d_{11}^{(2)}$. Let us introduce $\alpha_2 = C_{44}^{(2)}/C_{44}^{(1)}$, $\beta_2 = e_{15}^{(2)}/e_{15}^{(1)}$ and $\lambda_2 = x_0/R$. The normalized force F_{xo2} on dislocation versus θ is depicted in Fig. 7 with different β_2 for $\alpha_2 = 1$ and $\lambda_2 = 0.8$. It is seen that image force is equal to zero in homogeneous piezoelectric material as $\theta = 0$ and $\beta_2 = 1$. F_{xo2} is always negative as $\beta_1 > 1$, for which the piezoelectric matrix repel dislocation located inside inhomogeneity. For $\beta_1 < 1$, F_{xo1} is positive first, and then becomes negative. The image force will increase with the increase

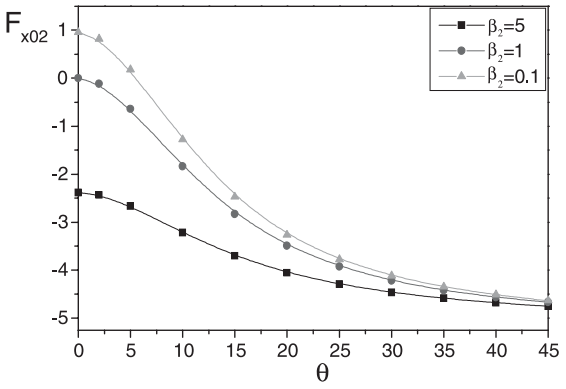

Fig. 7. Normalized force F_{xo2} versus θ with different β_2 for $\alpha_2 = 1$ and $\lambda_2 = 0.8$.

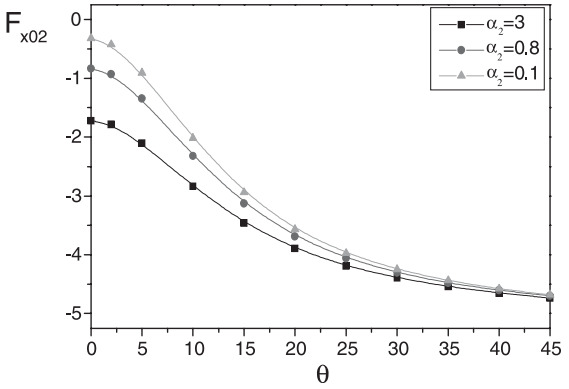

Fig. 8. Normalized force F_{xo2} versus θ with different α_2 for $\beta_2 = 2$ and $\lambda_2 = 0.8$.

of rigid line angle θ which indicates interfacial rigid line repel screw dislocation located inside inhomogeneity. The variation of the normalized force F_{xo2} acting on dislocation with rigid line angle θ is plotted in Fig. 8 with different α_2 for $\beta_2 = 2$ and $\lambda_2 = 0.8$. Noticeable, F_{xo2} is negative as $\theta = 0$ and $\alpha_2 = 0.1$, 0.8 which shows soft matrix can repel dislocation in piezoelectric materials. To our knowledge, soft matrix will attract dislocation inside inhomogeneity all along in non-piezoelectric composites. It is also shown that F_{xo2} will decrease with the increase of rigid line radian for which rigid line always repel dislocation. In Fig. 9, we illustrate variation of normalized force F_{xo2} versus λ_2 with different value of β_2 for $\alpha_2 = 1$ and $2\theta = 20°$. It is found that $F_{xo2} < 0$ due to the presence of interfacial rigid line inclusion when dislocation is located at origin. Further, It is seen that the normalized force F_{xo2} is always negative as $\beta_2 > 1$. For $\beta_2 < 1$, matrix and rigid line inclusion attract dislocation first, and then repel it. In spite of getting any value of β_2, the magnitude of repulsion force on dislocation will be a negative large value when dislocation approaches to rigid line inclusion ($\lambda_2 \to 1$) from origin alongwith x-axis. The variation of the normalized force F_{xo2} with λ_2 is plotted in Fig. 10 with different α_2 for $2\theta = 20°$ and $\beta_2 = 1$. It is shown that F_{xo2} is always negative when $\alpha_2 > 1$ (hard matrix), for which hard matrix and rigid line inclusion always repel dislocation located inside inhomogeneity. When $\alpha_2 < 1$ (soft matrix), the normalized force F_{xo2} will increase first, and then decrease as dislocation approaches to rigid line inclusion from origin along with x-axis. In spite of $\alpha_2 > 1$ or $\alpha_2 < 1$, the value of attraction force on dislocation will be a negative large value when dislocation approaches to rigid

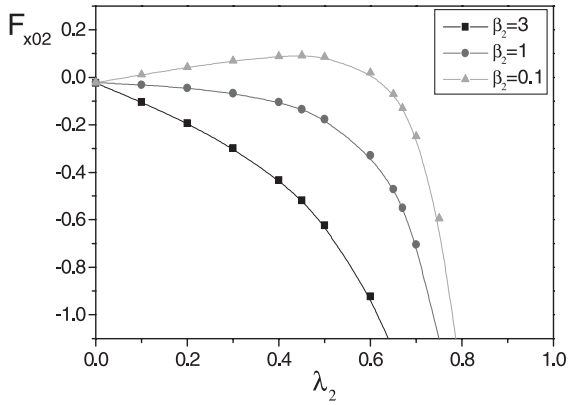

Fig. 9. Normalized force F_{xo2} versus λ_2 with different β_2 for $\alpha_2 = 1$ and $\theta = 10°$.

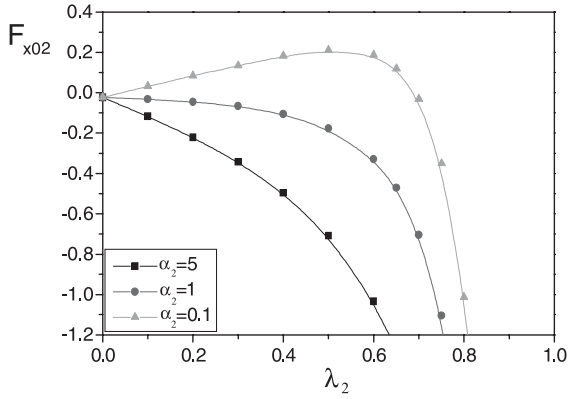

Fig. 10. Normalized force F_{xo2} versus λ_2 with different α_2 for $\beta_2 = 1$ and $\theta = 10°$.

line inclusion. In Fig. 9 or Fig. 10, when $\beta_2 < 1$ or $\alpha_2 < 1$, there may be two stable equilibrium positions or no equilibrium point along x-axis which depend on combinations of shear modulus ratio α_2, piezoelectric modulus ratio β_2 and rigid line angle θ.

7. Conclusions

Using Muskhelishvili's complex variable method, the closed form complex potentials are obtained for a piezoelectric screw dislocation located either inside matrix or inhomogeneity interacting with interfacial rigid line inclusions in this paper. Analytical expressions of image force on dislocation are also given. In Section 6, influence of rigid line geometrical dimension and materials elastic constants on dislocation force is discussed in graph. The results indicate interfacial rigid line play an important role in the interaction dislocation force. The obtained explicit solutions of Eqs. (43), (44) and (50), (51) can be used as Green's functions to solve the problem of interaction between interfacial rigid lines and arbitrary shape crack inside matrix or inhomogeneity under anti-plane mechanical and in-plane electric loadings at infinite.

Acknowledgements

The authors would like to thank the support by National Natural Science Foundation of China and the Natural Science Foundation of Hunan Province.

References

Deng, W., Meguid, S.A., 1999. Analysis of a screw dislocation inside an elliptical inhomogeneity in piezoelectric solids. International Journal of Solids and Structures 36, 1449–1469.

Hirth, J.P., Lothe, J., 1982. Theory of Dislocations, second ed. John-Wiley, New York.

Huang, Z., Kuang, Z.B., 2001. Dislocation inside a piezoelectric media with an elliptical inhomogeneity. International Journal of Solids and Structures 38, 8459–8480.

Jiang, C.P., Tong, Z.H., Chueng, Y.K., 2001. A generalized self-consistent method for piezoelectric fiber reinforced composites under anti-plane shear. Mechanics of Materials 33, 295–308.

Kattis, M.A., Providas, E., Kalamkarov, A.L., 1998. Two-phone potentials in the analysis of smart composites having piezoelectric components. Composites Part B 29 (1), 9–14.

Lee, K.Y., Lee, W.G., Pak, Y.E, 2000. Interaction between a semi-infinite crack and a screw dislocation in a piezoelectric material. ASME Journal of Applied Mechanics 67, 165–170.

Liu, Y.W., 1991. Base singular solutions of anti-plane problem on circular-arc cracks between bonded dissimilar materials. ACTA Mechanica Solids Sinica 12, 244–254.

Liu, J.X., Jiang, Z.Q., Feng, W.J., 2000. On the electro-elastic interaction of piezoelectric screw dislocation with an elliptical inclusion in piezoelectric materials. Applied Mathematics and Mechanics 21, 1185–1190.

Meguid, S.A., Deng, W., 1998. Electro-elastic interaction between a screw dislocation and elliptical inhomogeneity in piezoelectric materials. International Journal Solids and Structures 35, 1467–1482.

Meggiud, S.A., Zhong, Z., 1997. Electroelastic analysis of a piezoelectric elliptical inhomogeneity. International Journal of Solids and Structures 34, 3401–3414.

Muskhelishvili, N.L., 1975. Some Basic problems of Mathematical Theory of Elasticity. Noordhoff, Leyden.

Pak, Y.E., 1990. Force on piezoelectric screw dislocation. ASME, Journal of Applied Mechanics 57, 863–869.

Pak, Y.E., 1992. Circular inclusion problem in anti-plane piezoelectricity. International Journal of Solids and Structures 29, 2403–2419.

Smith, E., 1968. The interaction between dislocation and inhomogeneities-1. International Journal of Engineering Science 6, 129–143.

Tiersten, H.F., 1969. Linear Piezoelectric Plate Vibrations. Plenum Press, New York.

Toya, 1974. A crack along the interface of a circular inclusion embedded in an infinite solid. Journal of Mechanics and Physics of Solids 22, 325–348.

Zhang, T.Y., Qian, C.F., 1996. Interaction of a screw dislocation with a thin-film covered mode III crack. Acta Metallurgica et Materialia 39, 2739–2744.

Zhang, T.Y., Zhao, M., Tong, P., 2001. Fracture of Piezoelectric ceramics. Advances in Applied Mechanics 38, 147–289.

Zhong, Z., Meggiud, S.A., 1997. Interfacial debonding of circular inhomogeneity in piezoelectric materials. International Journal of Solids and Structures 34, 1965–1983.